

Characterization of kinase inhibitors using different phosphorylation states of colony stimulating factor-1 receptor tyrosine kinase

Received June 20, 2011; accepted August 20, 2011; published online August 31, 2011

Daisuke Kitagawa^{1,*}, Masaki Gouda¹,
Yasuyuki Kirii¹, Naoyuki Sugiyama²,
Yasushi Ishihama^{2,3}, Ikuo Fujii⁴,
Yugo Narumi¹, Kensaku Akita¹ and
Koichi Yokota¹

¹Carna Biosciences, Inc, 1-5-5, Minatojima-Minamimachi, Chuo-ku, Kobe 650-0047, ²Institute for Advanced Biosciences, Keio University, Daihoji, Tsuruoka, Yamagata 997-0017, ³Department of Molecular and Cellular BioAnalysis, Graduate School of Pharmaceutical Sciences, Kyoto University, Sakyo-ku, Kyoto 606-8501, and ⁴Department of Biological Science, Graduate School of Science, Osaka Prefecture University, 1-1, Gakuencho, Naka-ku, Sakai 599-8531, Japan

*Daisuke Kitagawa, Carna Biosciences, Inc, 1-5-5, Minatojima-Minamimachi, Chuo-ku, Kobe 650-0047, Japan. Tel: +81 78 302 7040, Fax: +81 78 302 7086, email: daisuke.kitagawa@carnabio.com

It is known that some kinase inhibitors are sensitive to the phosphorylation state of the kinase, and therefore those compounds can discriminate between a phosphorylated and unphosphorylated protein. In this study, we prepared two colony stimulating factor-1 receptor (CSF-1R) tyrosine kinase proteins: one highly phosphorylated by autophosphorylation and the other dephosphorylated by phosphatase treatment. These kinases were subjected to an activity-based assay to investigate the effect of their phosphorylation state on the potency of several kinase inhibitors. Dasatinib, sorafenib, PD173074 and staurosporine showed similar inhibition against different phosphorylation states of CSF-1R, but pazopanib, sunitinib, GW2580 and imatinib showed more potent inhibition against dephosphorylated CSF-1R. Binding analysis of the inhibitors to the two different phosphorylation forms of CSF-1R, using surface plasmon resonance spectrometry, revealed that staurosporine bound to both forms with similar affinity, but sunitinib bound to the dephosphorylated form with higher affinity. Thus, these observations suggest that sunitinib binds preferentially to the inactive form, preventing the activation of CSF-1R. Screening against different activation states of kinases should be an important approach for prioritizing compounds and should facilitate inhibitor design.

Keywords: CSF-1R/drug design/kinase inhibitor/phosphorylation/tyrosine kinase.

Abbreviations: CML, chronic myeloid leukaemia; CSF-1, colony stimulating factor-1; CSF-1R, colony stimulating factor-1 receptor; D-CSF-1R, dephosphorylated CSF-1R; P-CSF-1R, phosphorylated CSF-1R; RTK, receptor tyrosine kinase; Sf,

Spodoptera frugiperda; VEGFR, vascular endothelial growth factor receptor; λPPase, lambda phosphatase.

There are 518 kinases encoded in the human genome including serine/threonine, tyrosine and dual specific kinases (1, 2). Due to the pivotal roles in virtually all aspects of cellular physiology, the dysregulation of kinase activity-related signalling is involved in many kinds of diseases, such as cancer, inflammation and neurodegeneration (3, 4). Therefore, protein kinases have become one of the most important target classes for drug discovery (5). So far, 10 small-molecular weight tyrosine kinase inhibitors have been approved for cancer treatment and >100 kinase inhibitors are at present in clinical development (6–8). The majority of these inhibitors compete with ATP on binding to the ATP-binding pocket. Due to the entity of over 500 protein kinases in the human genome and the structural similarity of the kinase ATP sites, generally they inhibit multiple kinases simultaneously (2).

To understand the efficacy and side effects of the kinase inhibitors, it is important to know their target and off-target kinases (9, 10). Many tyrosine kinases sample diverse conformations between active and inactive forms, which are regulated by phosphorylation and dephosphorylation in physical or pathological conditions. It is known that some kinase inhibitors are sensitive to the phosphorylation state of the kinase, and therefore those compounds can discriminate between phosphorylated and dephosphorylated proteins (11, 12). However, the biological consequences of this phosphorylation sensitivity are poorly defined. Profiling against different phosphorylation states of kinases should be an important approach for better understanding the efficacy of kinase inhibitors and prioritizing them. In this study, we addressed colony stimulating factor-1 receptor (CSF-1R) for the profiling.

CSF-1R is a type III receptor tyrosine kinase (RTK), encoded by the *c-fms* proto-oncogene, and it is the exclusive receptor for macrophage colony stimulating factor 1 (CSF-1) (13). Together with CSF-1, CSF-1R regulates proliferation, differentiation and survival of cells of the mononuclear phagocyte lineage and prostate development (14–17). CSF-1 binding to the CSF-1R extracellular domain induces dimerization and trans-autophosphorylation of the intracellular CSF-1R kinase domain on several tyrosine residues (18). RTKs, including CSF-1R contain activation loop,

comprise a string of ~22 amino acids that begins with a protein kinase-conserved Asp-Phe-Gly (DFG) motif and ends with a Pro that is conserved among tyrosine kinases (19). At least one phosphorylation site resides at centre of activation loop, and its phosphorylation stimulates an outward movement of the activation loop. This movement induces the rotating of the DFG motif into proper orientation (DFG-in) for catalysis (20). Tyr-809 is a unique tyrosine residue in the activation loop of CSF-1R, and its phosphorylation is known to be important for kinase activity (21). The protein structures of active (DFG-in) and inactive (DFG-out) forms of the CSF-1R kinase domain have been reported (22–24). In order to evaluate the inhibitory potencies of protein inhibitors against the active and inactive forms of CSF-1R, we prepared two different CSF-1R tyrosine kinase proteins: one highly phosphorylated by autophosphorylation and the other dephosphorylated by phosphatase treatment. And then we established the kinase assay using these two types of CSF-1R.

The clinically relevant RTK inhibitors imatinib, dasatinib, pazopanib, sorafenib and sunitinib, and the well known kinase inhibitors staurosporine, GW2580 and PD173074 (25) are known to associate with CSF-1R (9). Imatinib and dasatinib are used for treatment of Philadelphia chromosome-positive chronic myeloid leukaemia (CML) with the chimeric gene BCR-ABL and KIT-positive gastrointestinal stromal tumour through inhibition of tyrosine kinases (26, 27); dasatinib is used for treatment of imatinib-resistant or -intolerant CML patients (28). Imatinib has been demonstrated to have potent inhibition only against the inactive (dephosphorylated) form of ABL (29), but dasatinib shows potent inhibition also against the active form of ABL (30). Sorafenib, sunitinib and pazopanib are used for treatment of patients with advanced renal cell carcinoma through inhibition of multiple RTKs, including vascular endothelial growth factor receptor (VEGFR) tyrosine kinases, which are involved in aberrant tumour angiogenesis (31–33). In this study, we investigated the effects of these kinase inhibitors on dephosphorylated and hyperphosphorylated forms of CSF-1R.

Materials and Methods

Reagents

Staurosporine and GW2580 were purchased from Calbiochem (San Diego, CA, USA), PD173074 was from Tocris (Bristol, UK), and pazopanib was from LC laboratories (Woburn, MA, USA). Sunitinib (34), dasatinib (35) and sorafenib (36) were synthesized at Carna Biosciences, Inc (Kobe, Japan). Imatinib mesylate (imatinib) was extracted from its pharmaceutical capsule. Triton X-100 and HEPES were purchased from Sigma-Aldrich (MO, USA), and the other reagents were from Wako Pure Chemical Industries (Osaka, Japan). FITC-labelled peptide substrate was purchased from Peptide Institute (Osaka, Japan).

Plasmid construction

The regions encoding the cytoplasmic domain of human CSF-1R (NM_005211.3, amino acids 538–972) fused with N-terminal His₆-tag and C-terminal biotin-accepting peptide, and BirA biotin-protein ligase (37) were subcloned into pFastBAC dual (Invitrogen, Carlsbad, CA, USA). The recombinant bacmid DNA was prepared according to the instructions for the Bac-to-Bac baculovirus expression system (Invitrogen) and transfected to *Spodoptera frugiperda* (Sf) 9 insect cells to amplify the recombinant

baculovirus. The titre of amplified baculovirus was determined by BacPAK Baculovirus Rapid Titer Kit (Takara, Shiga, Japan).

Protein expression and purification

To express CSF-1R, Sf21 cells (2×10^6 cells/ml) in Grace's insect media supplemented with 10% FCS were infected with the recombinant baculovirus at a multiplicity of infection of three and cultured for 48 h at 27°C. The cells were harvested, washed with cold PBS buffer and stored at –80°C until purification. The frozen cells were thawed and lysed in lysis buffer (50 mM Tris–HCl, pH 7.5, 300 mM NaCl, 10 mM imidazole, 1% Nonidet P-40, 5 mM DTT, 1 mM phenylmethanesulfonyl fluoride, 2 µg/ml leupeptin and 2 µg/ml aprotinin) on ice. All purification procedures thereafter were carried out at 4°C. The cell lysate was clarified by centrifugation at 9,000 g for 20 min and mixed with Ni-NTA Superflow resins (Qiagen, Tokyo, Japan). The lysate–resin mixture was packed in a column and washed with five volumes of wash buffer (50 mM Tris–HCl, pH 7.5, 1 M NaCl, 20 mM imidazole and 10% glycerol). CSF-1R was eluted with elution buffer (50 mM Tris–HCl, pH 7.5, 300 mM NaCl, 250 mM imidazole and 10% glycerol), and the CSF-1R-containing fractions were pooled. The eluted protein was divided into aliquots: one was autophosphorylated by incubation with 3 mM ATP and 10 mM MgCl₂ at 4°C overnight, and another was dephosphorylated by incubation with 10 U/µg-protein lambda phosphatase (λPPase; New England Biolabs, MA, USA) at 4°C overnight. The autophosphorylated CSF-1R (P-CSF-1R) and dephosphorylated CSF-1R (D-CSF-1R) were separated from the ATP and λPPase by chromatography, respectively.

Protein identification

The CSF-1R protein was applied to SDS–PAGE followed by Coomassie brilliant blue (CBB) staining. The band corresponding to CSF-1R was excised and analysed by matrix-assisted laser desorption/ionization reflection time-of-flight (MALDI-TOF) mass spectrometry (MS). The peptide mass analysis of trypsin-digested peptide was performed on autoflex III MALDI-TOF MS (Bruker, Yokohama, Japan) as previously described (38). Peptide identification was accomplished using MASCOT Peptide Mass Fingerprinting.

Protein phosphorylation analysis

To analyse the phosphorylation state, CSF-1R protein was digested with Lys-C and trypsin as previously described (39, 40), and the following NanoLC-MS/MS analyses were conducted using an Orbitrap system (LTQ-Orbitrap XL; Thermo Fisher Scientific, Bremen, Germany), Dionex Ultimate3000 pump with FLM-3000 flow manager (Germering, Germany), HTC-PAL autosampler (CTC Analytics, Zwingen, Switzerland), an analytical column needle with 'stone-arch' frit and a PTFE-coated column holder (Nikkyo) (41). The digested sample (5 µl) was injected and separated by a three-step gradient (41). The spray voltage was 2400 V, the MS scan range was *m/z* 300–1400 and the top 10 precursor ions were selected for subsequent MS/MS scans. A lock mass function was used for the LTQ-Orbitrap to obtain constant mass accuracy during gradient analysis (42). Peptides and proteins were identified by means of automated database searching using Mascot v2.2 (Matrix Science, London, UK) against SwissProt release 2010_06 (18-May-2010) (43). Phosphorylation sites were unambiguously determined when b- or y-ions, which were between the existing phosphorylated residues, were observed in the peak list of fragment ions. Quantitative analyses of phosphorylated and non-phosphorylated peptides derived from CSF-1R were carried out by a label-free approach (44–46). Phosphorylation stoichiometry was calculated based on relative peak areas of phosphorylated peptides and non-phosphorylated peptides according to the literature (47), with the modification that the peak area ratio was estimated with the label-free approach instead of stable isotope labelling by amino acids in cell culture (SILAC) method (48).

Activity-based kinase assay

CSF-1R kinase activity was determined by off-chip mobility shift assay (MSA) using LabChipTM3000 (Caliper Life Sciences, Hopkinton, MA, USA). The kinase, FITC-labelled peptide substrate (1 µM) named Srcide (49), and compound or vehicle (1% DMSO) were incubated in assay buffer (20 mM HEPES, pH 7.5, 0.01% Triton X-100, 2 mM DTT, 5 mM MgCl₂ and 1 mM ATP) at 25°C. The amounts (peak height) of phosphorylated (P) and non-phosphorylated (S) peptide substrates were measured and the

phosphorylation rate of the substrate was defined by $P/(P+S)$. To determine the IC_{50} value, each compound was diluted in DMSO in half-log scale and incubated with CSF-1R kinases for 10 min before the kinase reaction. The kinase reaction (20 μ l) was terminated by the addition of 60 μ l of termination buffer (127 mM HEPES, pH 7.5, 0.01% Triton X-100, 26.7 mM EDTA-2Na, 1% DMSO and 0.13% Coating-3 Reagent). The inhibition percentage of each compound against kinase activity was determined from the phosphorylation percentage of the substrate and the IC_{50} value was calculated by interpolation on a log-concentration-response curve fitting for four-parameter logistic equation.

Interaction between CSF-1R and kinase inhibitors

The interaction between CSF-1R and the kinase inhibitors was determined by surface plasmon resonance (SPR) using Biacore T100 (GE Healthcare, UK). The instrument running buffer was composed of 50 mM Tris-HCl, pH 7.5, 150 mM NaCl, 10 mM $MgCl_2$, 0.05% Tween-20 and 2% DMSO, which was also used as sample dilution buffer. Immobilization of CSF-1R protein onto a streptavidin-coated sensor chip SA (GE Healthcare) was performed according to the immobilization wizard in the Biacore instrument control software, including the following steps: (i) wash with 50 mM NaOH/1 M NaCl for 30 s, three times; (ii) injection of kinases for 15–20 min at 30 μ g/ml in running buffer and (iii) surface blockage with 10 μ g/ml EZ-LinkTM Biocytin (Thermo Fisher Scientific, Yokohama, Japan). Compounds were dissolved in DMSO at 10 mM, diluted with running buffer (50 mM Tris-HCl, pH 7.5, 150 mM NaCl, 10 mM $MgCl_2$, 0.05% Tween-20 and 2% DMSO) and analysed using a 2-fold dilution series. Interaction analysis cycles consisted of a 60 s sample injection (30 μ l/min) followed by 300 s of buffer flow (dissociation phase). All of the bound complexes dissociated back to baseline within a reasonable time frame, and regeneration was required. All sensorgrams were processed by subtracting the binding response recorded from the control surface (centre reference spot), followed by subtracting an average of the buffer blank injections from the reaction spot. To determine the kinetic rate constant, all data sets were fit to a simple 1:1 interaction model, including a term for mass transport using numerical integration and nonlinear curve fitting. Equilibrium analysis was performed by fitting the response at the end of the association phase to a single-site binding isotherm.

Results

Phosphorylation state of CSF-1R

Human recombinant CSF-1R protein was expressed and purified from insect cells, and was subsequently either autophosphorylated by treatment with ATP or dephosphorylated by λ PPase. CBB staining of these CSF-1R proteins is shown in Fig. 1A. A prominent band of CSF-1R was apparent at \sim 55 kDa, and the band of P-CSF-1R showed a slight upward shift from the position of non-treated CSF-1R and D-CSF-1R. To quantify the phosphorylation state of these CSF-1R proteins, LC-MS/MS analysis of tryptic digest of these proteins was carried out. As shown in Table I, the phosphorylation rates of five tyrosine residues (Y561, Y699, Y809, Y873 and Y923) were determined. Y809 is a unique tyrosine residue in the activation loop and considered to be one of the key residues for the kinase activity of CSF-1R (21). The phosphorylation rate of this residue in non-treated CSF-1R was 2.2%. In P-CSF-1R, the phosphorylation rate of Y809 was dramatically increased to 61.4%, and in D-CSF-1R it was negligible (0.2%). Tyrosine residues, Y561, Y699 and Y923, had high phosphorylation rates (>90%) in P-CSF-1R and low (<5%) phosphorylation rates in D-CSF-1R. In contrast, the phosphorylation rate of Y873 was increased by only 7% after autophosphorylation.

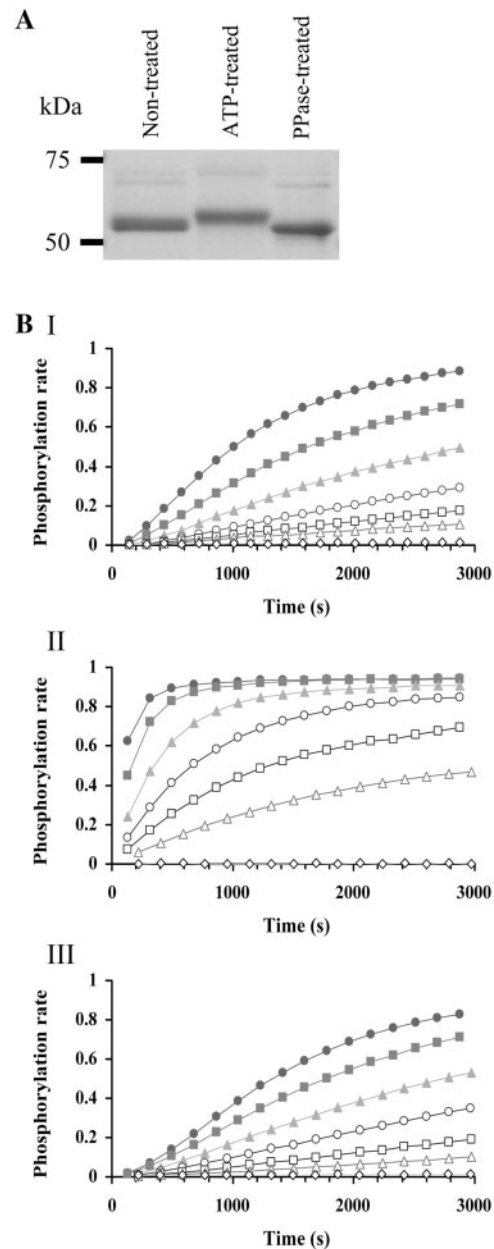


Fig. 1 Phosphorylation state and activity of different preparations of CSF-1R: (A) non-treated, autophosphorylated and λ PPase-treated CSF-1R proteins were subjected to SDS-PAGE followed by CBB staining. Migration positions of protein molecular mass standards (kDa) and bands corresponding to the expected protein size are indicated. The autophosphorylated CSF-1R protein showed a slight upward shift compared with the non-treated and λ PPase-treated proteins. (B) The kinase activity of (I) non-treated, (II) P- and (III) D-CSF-1R towards the Src peptide was evaluated using the activity-based assay. The ratio of the phosphorylated peptide was measured in a time-series at 1 mM ATP. Regarding non-treated and D-CSF-1R, a slight lag time in the phosphorylation of the peptide was observed at the beginning of the assay. The concentrations of CSF-1R kinases were 250 ng/ml (filled circle), 125 ng/ml (filled square), 62.5 ng/ml (filled triangle), 31.3 ng/ml (open circle), 15.6 ng/ml (open square) and 7.8 ng/ml (open triangle).

Kinase activity of CSF-1R

Analysis of the phosphorylation state of Y809 revealed that P-CSF-1R could be an active form and D-CSF-1R could be an inactive form of the kinase. The kinase activity of these CSF-1R proteins, determined by their

ability to phosphorylate the substrate peptide, was measured using the off-chip MSA. The phosphorylation rate of the substrate was monitored for 50 min from initiation of the kinase reaction (Fig. 1B). P-CSF-1R showed a time- and dose-dependent increase in the phosphorylation rate of the substrate, and its activity was ~10-fold higher than non-treated CSF-1R (Fig. 1B I and II). In contrast, D-CSF-1R showed slightly weaker kinase activities than the non-treated CSF-1R and had a short lag of about 10 min, indicating that D-CSF-1R might be activated to some degree during the kinase reaction (Fig. 1B III). The plots of the initial velocities versus ATP concentrations and fitting to the Michaelis–Menten equation revealed that the K_m value for ATP of P-CSF-1R was 37 μM (Fig. 2A). On the other hand, the velocity of D-CSF-1R could not reach the maximum even at 1,000 μM ATP (Fig. 2B).

CSF-1R kinase inhibition by tyrosine kinase inhibitors

To clarify the preference of eight tyrosine kinase inhibitors for the phosphorylation states of CSF-1R, their inhibitory effects on P- and D-CSF-1R were evaluated in the presence of 1 mM ATP (physiological concentration). P-CSF-1R (8 ng/ml) and D-CSF-1R (40 ng/ml), which could reach ~30% of substrate

phosphorylation rate 1 h after initiation of the assay, were used to determine the IC_{50} values. All compounds exhibited concentration-dependent inhibition of both forms of CSF-1R (Fig. 3, Table II). GW2580, pazopanib and sunitinib exhibited a clear preference (>10-fold) for D-CSF-1R, and imatinib tended to prefer D-CSF-1R to P-CSF-1R. Dasatinib, sorafenib, staurosporine and PD173074 inhibited both forms of CSF-1R in a similar manner. These findings indicate that GW2580, pazopanib, sunitinib and imatinib could easily bind to D-CSF-1R and in turn inhibit its activation; however, dasatinib, sorafenib, staurosporine and PD173074 could bind both forms of CSF-1R and inhibit its activity.

Binding affinity of sunitinib and staurosporine for CSF-1R

To investigate whether sunitinib has a higher affinity for D-CSF-1R than P-CSF-1R, the interaction of the compounds with CSF-1R protein was determined using SPR-based Biacore T100 technology. As the CSF-1R proteins have a biotinylated peptide sequence at the carboxyl-terminal, it is possible to immobilize the proteins readily onto a sensor chip utilizing the high affinity biotin-streptavidin system. Both D-CSF-1R and P-CSF-1R proteins were immobilized on a streptavidin-coated sensor chip and washed until a stable baseline was achieved. The qualitative plots of the association and dissociation patterns of sunitinib and staurosporine with the CSF-1R protein are shown in Fig. 4. To obtain the association and dissociation rate constants, various concentrations of the inhibitors were injected over the CSF-1R surface, ranging from 47 to 3,000 nM for sunitinib and from 3.1 to 300 nM for staurosporine. From the sensorgrams for each compound, association and dissociation rates were determined and K_D values were calculated for sunitinib and staurosporine (Table III). Two independent experiments showed that the average dissociation constant (K_D) of sunitinib was significantly lower for D-CSF-1R (87 nM) compared with P-CSF-1R (320 nM), whereas the K_D value of staurosporine for

Table I. Phosphorylation rate of CSF-1R protein kinase was determined using LC-MS/MS.

	Phosphorylation rate (%) ^a		
	Non-treated	Autophosphorylated	λPPase treated
Y561	15.1	95.8	3.2
Y699	2.3	93.5	0.1
Y809	2.2	61.4	0.2
Y873	2.6	9.7	0
Y923	0.6	94.2	0.1

^aTo quantify the phosphorylation rate of differently prepared CSF-1R proteins, LC-MS/MS analysis of tryptic digest of these proteins was carried out. The phosphorylation rates of five tyrosine residues are indicated.

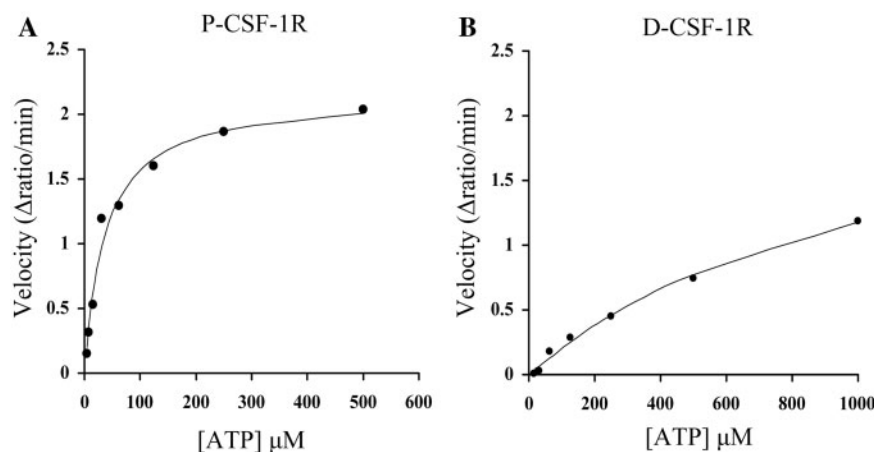


Fig. 2 Michaelis–Menten curves for ATP. (A) P-CSF-1R kinase was assayed at various concentrations of ATP, the initial velocity (V_i) was plotted against the concentration of ATP, and the K_m value was calculated. (B) D-CSF-1R kinase was assayed as described for (A). The concentrations of the CSF-1R proteins were 8 ng/ml for P-CSF-1R and 50 ng/ml for D-CSF-1R.

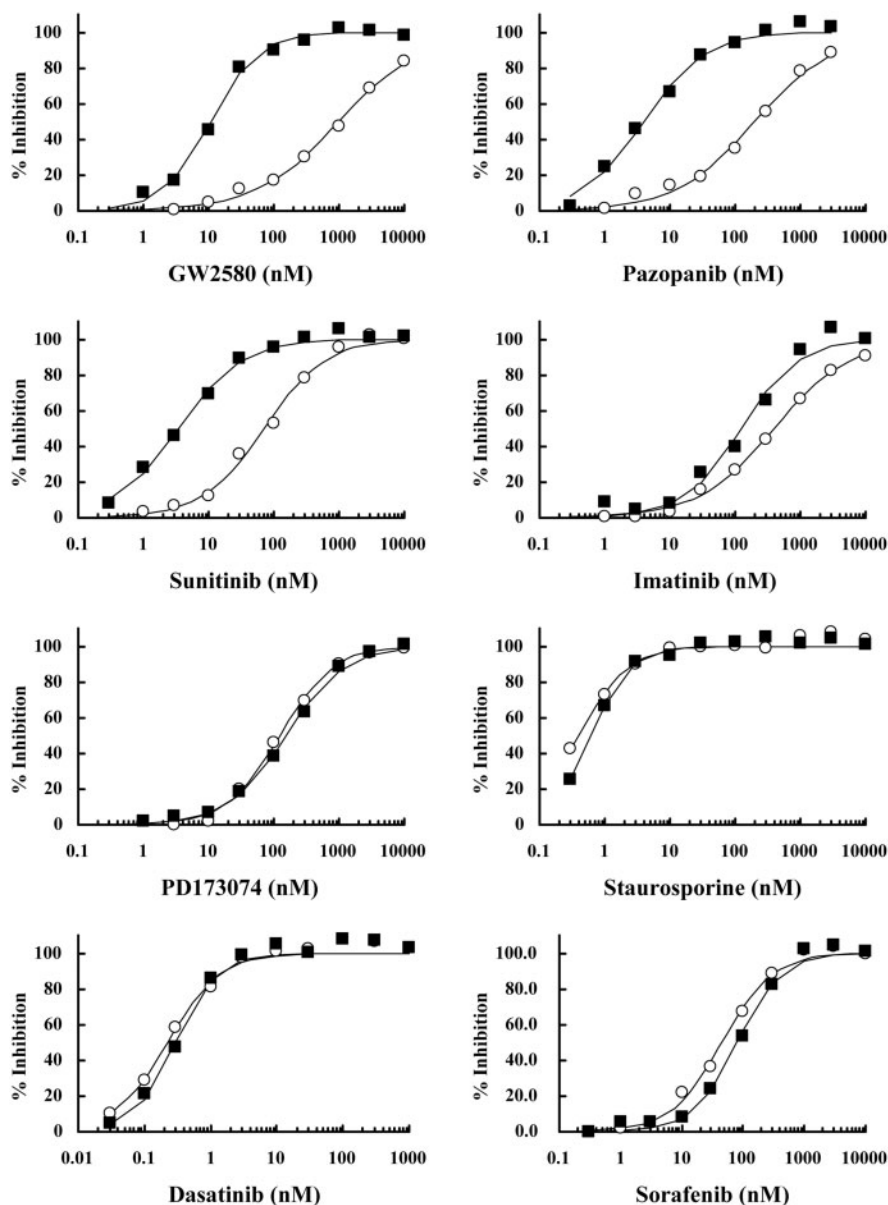


Fig. 3 Potency of tyrosine kinase inhibitors on different phosphorylation states of CSF-1R protein kinases. The kinase reaction was performed in the presence of the indicated concentrations of the inhibitors. Shown here is the inhibition percentage as a function of compound concentration. Data for P-CSF-1R are shown in open circles, and D-CSF-1R in filled squares. Representative curves are shown, and average IC_{50} values from at least two independent experiments are shown in Table II.

Table II. Potency of tyrosine kinase inhibitors measured by the activity-based assay.

Compound name	IC_{50} (nM) against CSF-1R ^a	
	P-CSF-1R	D-CSF-1R
GW2580	1100	11
Pazopanib	230	4.2
Sunitinib	79	3.8
Imatinib	370	110
PD173074	120	170
Staurosporine	0.44	0.74
Dasatinib	0.18	0.33
Sorafenib	43	91

^a IC_{50} values (nM) of eight tyrosine kinase inhibitors against two different phosphorylation forms of CSF-1R tyrosine kinase are reported. The values indicate the IC_{50} values from experiments with a 10-min pre-incubation of compound and kinase. Each value is an average of at least two independent experiments.

D-CSF-1R (43 nM) was barely different from that of P-CSF-1R (41 nM). These results indicate that sunitinib has a higher affinity for D-CSF-1R, which is consistent with the results from the activity-based kinase assay.

Discussion

It is known that some kinase inhibitors are sensitive to the phosphorylation state of the kinase, and therefore those compounds can discriminate between a phosphorylated and unphosphorylated protein. Imatinib has been reported to preferentially inhibit the unphosphorylated form of ABL (50). This observation is explained by the fact that imatinib preferentially binds to the DFG-out conformation of ABL due to association

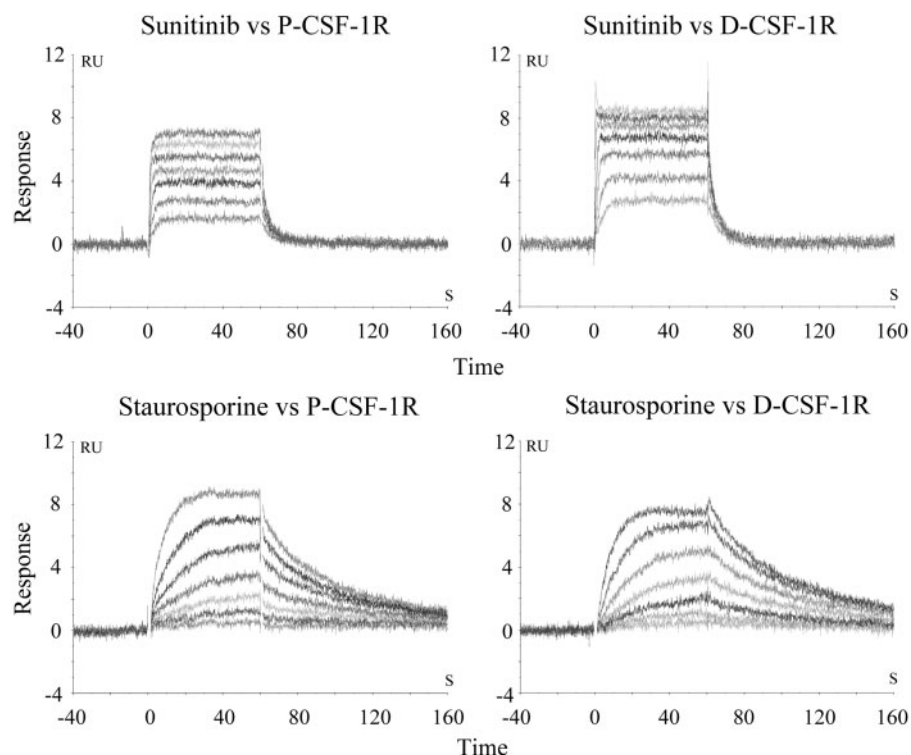


Fig. 4 Representative Biacore sensorgrams of sunitinib binding to D-CSF-1R and P-CSF-1R. To determine the affinities and kinetic constants, inhibitor concentrations above and below the K_D value were injected over immobilized CSF-1R. Sensorgrams of P-CSF-1R are shown in the left column and of D-CSF-1R in the right column. Staurosporine (3.1–300 nM) and sunitinib (47–3000 nM) were injected.

Table III. K_D values (nM) and kinetic rate constants of compounds were determined using Biacore T100.

Kinase	Inhibitor	k_a (1/Ms)	k_d (1/s)	K_D (nM) ^a	Assay conc. (nM)
P-CSF-1R	Sunitinib	1.5×10^6	0.47	320 (420)	47–3000
P-CSF-1R	Staurosporine	6.1×10^5	0.018	30 (53)	3.1–200
D-CSF-1R	Sunitinib	3.0×10^6	0.20	68 (100)	47–3000
D-CSF-1R	Staurosporine	3.6×10^5	0.016	44 (62)	4.7–300

^a K_D values (nM) were calculated by kinetics analysis of the sensorgrams shown in Fig. 3. The values in parenthesis indicate the K_D values from affinity analysis.

with the allosteric pocket adjacent to the ATP binding site. This pocket is made accessible by the activation-loop rearrangement that is characteristic of kinases in the inactive conformation (11). Kinase inhibitors such as imatinib and sorafenib are called type II inhibitors. On the other hand, staurosporine is classified into type I inhibitors that bind to the ATP binding site of the kinase in its active conformation. Although imatinib is known to bind the inactive forms of ABL, KIT, SRC and others (23), it binds an active conformation of SYK (51). The information provides a precedent that a tyrosine kinase inhibitor adopts different binding modes against different target kinase.

CSF-1R is a class III RTK and is the exclusive receptor for CSF-1. Binding of CSF-1 to the CSF-1R extracellular domain induces CSF-1R dimerization and trans-autophosphorylation of the intracellular CSF-1R kinase domain on several tyrosine residues, including tyrosine 561, 699, 708, 723 and 809 (52–54). In this study, we prepared two CSF-1R kinases: one was highly phosphorylated by

autophosphorylation and the other was dephosphorylated by λ PPase treatment. P-CSF-1R was phosphorylated on several tyrosine residues, including tyrosine 561, 699, 809 and 923. Tyrosine 561 in the juxtamembrane domain has been indicated to be engaged in the auto-inhibitory function (23), and the phosphorylated tyrosine acts as a binding site for SRC family tyrosine kinases (55). The phosphorylated Y699 is known as the binding site for Grb2 (56). Y809 is conserved in most tyrosine kinases, and its phosphorylation results in increased kinase activity (57). The phosphorylation of Y561 suggests that P-CSF-1R is relieved of the auto-inhibition, and the phosphorylation of Y809, the only tyrosine residue in the activation loop, indicates that the P-CSF-1R was highly activated. On the other hand, λ PPase treatment almost completely dephosphorylated all these tyrosine residues, indicating that D-CSF-1R was in an inactive form. The P-CSF-1R had a high catalytic activity and a higher affinity for ATP (lower K_m value). In contrast, D-CSF-1R was less active and had a lower affinity for ATP

(higher K_m value), confirming that P-CSF-1R was in the active form and D-CSF-1R was in the inactive form (Figs. 1 and 2).

The inhibitory potency of eight CSF-1R inhibitors on two different phosphorylation states of CSF-1R was determined in the presence of the physiological concentration (1 mM) of ATP. GW2580, pazopanib and sunitinib clearly showed higher inhibitory potencies on D-CSF-1R than P-CSF-1R. In the binding analysis using SPR, the K_D value of sunitinib for D-CSF-1R was lower than for P-CSF-1R (Fig. 4, Table III). GW2580 has been demonstrated to be an extremely selective inhibitor for CSF-1R and has been hypothesized to bind to the DFG-out mode of CSF-1R, which might lock it into an inactive conformation (24). Although sunitinib is known to be a type I inhibitor of various kinases, including VEGFR2 and PDGFR β (58, 59), it binds and inhibits inactive KIT that has similar amino acid sequences to CSF-1R around the ATP binding pocket (60). Sunitinib cannot be docked into the ATP binding pocket in the active CSF-1R model (61). The information supports the idea that GW2580 and sunitinib bound preferentially to the inactive form of CSF-1R and prevented its activation. Like GW2580 and sunitinib, pazopanib is also likely to bind and inhibit the inactive form of CSF-1R. Imatinib showed slightly potent inhibition against D-CSF-1R. It may be consistent with the previous report that imatinib has some steric binding clash in the autoinhibited conformation of CSF-1R (23). Thus, imatinib may not have such a strong preference for the CSF-1R inactive form.

Dasatinib, sorafenib, staurosporine and PD173074 inhibited both phosphorylation states of CSF-1R with similar IC_{50} values (Fig. 3 and Table II). Binding analysis of staurosporine to CSF-1R revealed that staurosporine had similar K_D values for the active and inactive forms (Fig. 4 and Table III). Staurosporine is a typical type I inhibitor that is supposed to bind and inhibit the active form of kinases. The docking analysis revealed that dasatinib was docked into the CSF-1R model with the active conformation (61). Although the active CSF-1R had higher affinity for ATP than the inactive form, dasatinib, sorafenib, staurosporine and PD173074 are likely to bind both active and inactive forms of CSF-1R and inhibit the kinase activity.

In summary, we established the activity-based assay by which potency of inhibitors against plural activation states of CSF-1R can be estimated. Such an approach should be applicable to other kinases, which may be important to assess efficacy of inhibitors and should facilitate kinase inhibitor design.

Acknowledgements

We thank all our colleagues at Carna Biosciences for valuable discussions.

Conflict of interest

None declared.

References

- Hunter, T. (2000) Signaling—2000 and beyond. *Cell* **100**, 113–127
- Manning, G., Whyte, D.B., Martinez, R., Hunter, T., and Sudarsanam, S. (2002) The protein kinase complement of the human genome. *Science* **298**, 1912–1934
- Hunter, T. (1998) The role of tyrosine phosphorylation in cell growth and disease. *Harvey Lect.* **94**, 81–119
- Cohen, P. (2002) Protein kinases—the major drug targets of the twenty-first century? *Nat. Rev. Drug Discov.* **1**, 309–315
- Zhang, J., Yang, P.L., and Gray, N.S. (2009) Targeting cancer with small molecule kinase inhibitors. *Nat. Rev. Cancer* **9**, 28–39
- Force, T. and Kolaja, K.L. (2011) Cardiotoxicity of kinase inhibitors: the prediction and translation of pre-clinical models to clinical outcomes. *Nat. Rev. Drug Discov.* **10**, 111–126
- Zsila, F., Fitos, I., Bencze, G., Keri, G., and Orfi, L. (2009) Determination of human serum alpha1-acid glycoprotein and albumin binding of various marketed and preclinical kinase inhibitors. *Curr. Med. Chem.* **16**, 1964–1977
- Puxeddu, E., Romagnoli, S., and Dottorini, M.E. (2011) Targeted therapies for advanced thyroid cancer. *Curr. Opin. Oncol.* **23**, 13–21
- Karaman, M.W., Herrgard, S., Treiber, D.K., Gallant, P., Atteridge, C.E., Campbell, B.T., Chan, K.W., Ciceri, P., Davis, M.I., Edeen, P.T., Faraoni, R., Floyd, M., Hunt, J.P., Lockhart, D.J., Milanov, Z.V., Morrison, M.J., Pallares, G., Patel, H.K., Pritchard, S., Wodicka, L.M., and Zarrinkar, P.P. (2008) A quantitative analysis of kinase inhibitor selectivity. *Nat. Biotechnol.* **26**, 127–132
- Graczyk, P.P. (2007) Gini coefficient: a new way to express selectivity of kinase inhibitors against a family of kinases. *J. Med. Chem.* **50**, 5773–5779
- Liu, Y. and Gray, N.S. (2006) Rational design of inhibitors that bind to inactive kinase conformations. *Nat. Chem. Biol.* **2**, 358–364
- Zuccotto, F., Ardini, E., Casale, E., and Angiolini, M. (2010) Through the ‘gatekeeper door’: exploiting the active kinase conformation. *J. Med. Chem.* **53**, 2681–2694
- Sherr, C.J., Rettenmier, C.W., Sacca, R., Roussel, M.F., Look, A.T., and Stanley, E.R. (1985) The c-fms proto-oncogene product is related to the receptor for the mononuclear phagocyte growth factor, CSF-1. *Cell* **41**, 665–676
- Stanley, E.R., Guilbert, L.J., Tushinski, R.J., and Bartelmez, S.H. (1983) CSF-1—a mononuclear phagocyte lineage-specific hemopoietic growth factor. *J. Cell. Biochem.* **21**, 151–159
- Ide, H., Seligson, D.B., Memarzadeh, S., Xin, L., Horvath, S., Dubey, P., Flick, M.B., Kacinski, B.M., Palotie, A., and Witte, O.N. (2002) Expression of colony-stimulating factor 1 receptor during prostate development and prostate cancer progression. *Proc. Natl Acad. Sci. USA* **99**, 14404–14409
- Hamilton, J.A. (2008) Colony-stimulating factors in inflammation and autoimmunity. *Nat. Rev. Immunol.* **8**, 533–544
- Chitu, V. and Stanley, E.R. (2006) Colony-stimulating factor-1 in immunity and inflammation. *Curr. Opin. Immunol.* **18**, 39–48

18. Bourette, R.P. and Rohrschneider, L.R. (2000) Early events in M-CSF receptor signaling. *Growth Factors* **17**, 155–166
19. Hubbard, S.R. (2002) Autoinhibitory mechanisms in receptor tyrosine kinases. *Front Biosci.* **7**, d330–340
20. Huse, M. and Kuriyan, J. (2002) The conformational plasticity of protein kinases. *Cell* **109**, 275–282
21. Davis, J.N., Rock, C.O., Cheng, M., Watson, J.B., Ashmun, R.A., Kirk, H., Kay, R.J., and Rousset, M.F. (1997) Complementation of growth factor receptor-dependent mitogenic signaling by a truncated type I phosphatidylinositol 4-phosphate 5-kinase. *Mol. Cell Biol.* **17**, 7398–7406
22. Schubert, C., Schalk-Hihi, C., Struble, G.T., Ma, H.C., Petrounia, I.P., Brandt, B., Deckman, I.C., Patch, R.J., Player, M.R., Spurlino, J.C., and Springer, B.A. (2007) Crystal structure of the tyrosine kinase domain of colony-stimulating factor-1 receptor (cFMS) in complex with two inhibitors. *J. Biol. Chem.* **282**, 4094–4101
23. Walter, M., Lucet, I.S., Patel, O., Broughton, S.E., Bamert, R., Williams, N.K., Fantino, E., Wilks, A.F., and Rossjohn, J. (2007) The 2.7 Å crystal structure of the autoinhibited human c-Fms kinase domain. *J. Mol. Biol.* **367**, 839–847
24. Meyers, M.J., Pelc, M., Kamtekar, S., Day, J., Poda, G.I., Hall, M.K., Michener, M.L., Reitz, B.A., Mathis, K.J., Pierce, B.S., Parikh, M.D., Mischke, D.A., Long, S.A., Parlow, J.J., Anderson, D.R., and Thorarensen, A. (2010) Structure-based drug design enables conversion of a DFG-in binding CSF-1R kinase inhibitor to a DFG-out binding mode. *Bioorg. Med. Chem. Lett.* **20**, 1543–1547
25. Mohammadi, M., Froum, S., Hamby, J.M., Schroeder, M.C., Panek, R.L., Lu, G.H., Eliseenkova, A.V., Green, D., Schlessinger, J., and Hubbard, S.R. (1998) Crystal structure of an angiogenesis inhibitor bound to the FGF receptor tyrosine kinase domain. *EMBO J.* **17**, 5896–5904
26. Ren, R. (2005) Mechanisms of BCR-ABL in the pathogenesis of chronic myelogenous leukaemia. *Nat. Rev. Cancer* **5**, 172–183
27. Demetri, G.D., von Mehren, M., Blanke, C.D., Van den Abbeele, A.D., Eisenberg, B., Roberts, P.J., Heinrich, M.C., Tuveson, D.A., Singer, S., Janicek, M., Fletcher, J.A., Silverman, S.G., Silberman, S.L., Capdeville, R., Kiese, B., Peng, B., Dimitrijevic, S., Druker, B.J., Corless, C., Fletcher, C.D., and Joensuu, H. (2002) Efficacy and safety of imatinib mesylate in advanced gastrointestinal stromal tumors. *N. Engl. J. Med.* **347**, 472–480
28. Shah, N.P., Tran, C., Lee, F.Y., Chen, P., Norris, D., and Sawyers, C.L. (2004) Overriding imatinib resistance with a novel ABL kinase inhibitor. *Science* **305**, 399–401
29. Schindler, T., Bornmann, W., Pellicena, P., Miller, W.T., Clarkson, B., and Kuriyan, J. (2000) Structural mechanism for STI-571 inhibition of abelson tyrosine kinase. *Science* **289**, 1938–1942
30. Tokarski, J.S., Newitt, J.A., Chang, C.Y., Cheng, J.D., Wittekind, M., Kiefer, S.E., Kish, K., Lee, F.Y., Borzilleri, R., Lombardo, L.J., Xie, D., Zhang, Y., and Klei, H.E. (2006) The structure of Dasatinib (BMS-354825) bound to activated ABL kinase domain elucidates its inhibitory activity against imatinib-resistant ABL mutants. *Cancer Res.* **66**, 5790–5797
31. Christensen, J.G. (2007) A preclinical review of sunitinib, a multitargeted receptor tyrosine kinase inhibitor with anti-angiogenic and antitumor activities. *Ann Oncol* **18** (Suppl. 10), x3–10
32. Kumar, R., Knick, V.B., Rudolph, S.K., Johnson, J.H., Crosby, R.M., Crouthamel, M.C., Hopper, T.M., Miller, C.G., Harrington, L.E., Onori, J.A., Mullin, R.J., Gilmer, T.M., Truesdale, A.T., Epperly, A.H., Bolor, A., Stafford, J.A., Luttrell, D.K., and Cheung, M. (2007) Pharmacokinetic-pharmacodynamic correlation from mouse to human with pazopanib, a multikinase angiogenesis inhibitor with potent antitumor and antiangiogenic activity. *Mol. Cancer Ther.* **6**, 2012–2021
33. Gotink, K.J. and Verheul, H.M. (2010) Anti-angiogenic tyrosine kinase inhibitors: what is their mechanism of action? *Angiogenesis* **13**, 1–14
34. Sun, L., Liang, C., Shirazian, S., Zhou, Y., Miller, T., Cui, J., Fukuda, J.Y., Chu, J.Y., Nematalla, A., Wang, X., Chen, H., Sistla, A., Luu, T.C., Tang, F., Wei, J., and Tang, C. (2003) Discovery of 5-[5-fluoro-2-oxo-1,2-dihydroindol-(3Z)-ylidenemethyl]-2,4-dimethyl-1H-pyrrole-3-carboxylic acid (2-diethylaminoethyl)amide, a novel tyrosine kinase inhibitor targeting vascular endothelial and platelet-derived growth factor receptor tyrosine kinase. *J. Med. Chem.* **46**, 1116–1119
35. Lombardo, L.J., Lee, F.Y., Chen, P., Norris, D., Barrish, J. C., Behnia, K., Castaneda, S., Cornelius, L.A., Das, J., Dowejko, A.M., Fairchild, C., Hunt, J.T., Inigo, I., Johnston, K., Kamath, A., Kan, D., Klei, H., Marathe, P., Pang, S., Peterson, R., Pitt, S., Schieven, G.L., Schmidt, R.J., Tokarski, J., Wen, M.L., Wityak, J., and Borzilleri, R.M. (2004) Discovery of N-(2-chloro-6-methyl-phenyl)-2-(6-(4-(2-hydroxyethyl)-piperazin-1-yl)-2-methylpyrimidin-4-ylamino)-thiazole-5-carboxamide (BMS-354825), a dual Src/Abl kinase inhibitor with potent antitumor activity in preclinical assays. *J. Med. Chem.* **47**, 6658–6661
36. Bankston, D., Dumas, J., Natero, R., Riedl, B., Monahan, M.-K., and Sibley, R. (2002) A potent Raf kinase inhibitor for the treatment of cancer. *Org. Proc. Res. Dev.* **6**, 777–781
37. Duffy, S., Tsao, K.L., and Waugh, D.S. (1998) Site-specific, enzymatic biotinylation of recombinant proteins in *Spodoptera frugiperda* cells using biotin acceptor peptides. *Anal Biochem.* **262**, 122–128
38. Kinoshita, T., Miyano, N., Nakai, R., Yokota, K., Ishiguro, H., and Tada, T. (2008) Protein purification and preliminary crystallographic analysis of human Lyn tyrosine kinase. *Protein Expr. Purif.* **58**, 318–324
39. Saito, H., Oda, Y., Sato, T., Kuromitsu, J., and Ishihama, Y. (2006) Multiplexed two-dimensional liquid chromatography for MALDI and nano-electrospray ionization mass spectrometry in proteomics. *J. Proteome Res.* **5**, 1803–1807
40. Rappsilber, J., Ishihama, Y., and Mann, M. (2003) Stop and go extraction tips for matrix-assisted laser desorption/ionization, nano-electrospray, and LC/MS sample pretreatment in proteomics. *Anal Chem.* **75**, 663–670
41. Ishihama, Y., Rappsilber, J., Andersen, J.S., and Mann, M. (2002) Microcolumns with self-assembled particle frits for proteomics. *J. Chromatogr. A* **979**, 233–239
42. Olsen, J.V., de Godoy, L.M., Li, G., Macek, B., Mortensen, P., Pesch, R., Makarov, A., Lange, O., Horning, S., and Mann, M. (2005) Parts per million mass accuracy on an Orbitrap mass spectrometer via lock mass injection into a C-trap. *Mol. Cell Proteomics* **4**, 2010–2021

43. Olsen, J.V., Ong, S.E., and Mann, M. (2004) Trypsin cleaves exclusively C-terminal to arginine and lysine residues. *Mol. Cell Proteomics* **3**, 608–614
44. Chelius, D. and Bondarenko, P.V. (2002) Quantitative profiling of proteins in complex mixtures using liquid chromatography and mass spectrometry. *J. Proteome Res.* **1**, 317–323
45. Ruse, C.I., Willard, B., Jin, J.P., Haas, T., Kinter, M., and Bond, M. (2002) Quantitative dynamics of site-specific protein phosphorylation determined using liquid chromatography electrospray ionization mass spectrometry. *Anal. Chem.* **74**, 1658–1664
46. Wang, G., Wu, W.W., Zeng, W., Chou, C.L., and Shen, R.F. (2006) Label-free protein quantification using LC-coupled ion trap or FT mass spectrometry: Reproducibility, linearity, and application with complex proteomes. *J. Proteome Res.* **5**, 1214–1223
47. Olsen, J.V., Vermeulen, M., Santamaria, A., Kumar, C., Miller, M.L., Jensen, L.J., Gnad, F., Cox, J., Jensen, T.S., Nigg, E.A., Brunak, S., and Mann, M. (2010) Quantitative phosphoproteomics reveals widespread full phosphorylation site occupancy during mitosis. *Sci. Signal.* **3**, ra3
48. Ong, S.E., Blagoev, B., Kratchmarova, I., Kristensen, D.B., Steen, H., Pandey, A., and Mann, M. (2002) Stable isotope labeling by amino acids in cell culture, SILAC, as a simple and accurate approach to expression proteomics. *Mol. Cell Proteomics* **1**, 376–386
49. Takano-Ohmuro, H., Yoshida, L.S., Yuda, Y., Morioka, K., and Kitani, S. (2008) Shikonin inhibits IgE-mediated histamine release by human basophils and Syk kinase activity. *Inflamm. Res.* **57**, 484–488
50. Nagar, B., Bornmann, W.G., Pellicena, P., Schindler, T., Veach, D.R., Miller, W.T., Clarkson, B., and Kuriyan, J. (2002) Crystal structures of the kinase domain of c-Abl in complex with the small molecule inhibitors PD173955 and imatinib (STI-571). *Cancer Res.* **62**, 4236–4243
51. Atwell, S., Adams, J.M., Badger, J., Buchanan, M.D., Feil, I.K., Froning, K.J., Gao, X., Hendle, J., Keegan, K., Leon, B.C., Muller-Dieckmann, H.J., Nienaber, V.L., Noland, B.W., Post, K., Rajashankar, K. R., Ramos, A., Russell, M., Burley, S.K., and Buchanan, S.G. (2004) A novel mode of Gleevec binding is revealed by the structure of spleen tyrosine kinase. *J. Biol. Chem.* **279**, 55827–55832
52. Rohrschneider, L.R., Bourette, R.P., Lioubin, M.N., Algate, P.A., Myles, G.M., and Carlberg, K. (1997) Growth and differentiation signals regulated by the M-CSF receptor. *Mol. Reprod. Dev.* **46**, 96–103
53. Flick, M.B., Sapi, E., Perrotta, P.L., Maher, M.G., Halaban, R., Carter, D., and Kacinski, B.M. (1997) Recognition of activated CSF-1 receptor in breast carcinomas by a tyrosine 723 phosphospecific antibody. *Oncogene* **14**, 2553–2561
54. Takeshita, S., Faccio, R., Chappel, J., Zheng, L., Feng, X., Weber, J.D., Teitelbaum, S.L., and Ross, F.P. (2007) c-Fms tyrosine 559 is a major mediator of M-CSF-induced proliferation of primary macrophages. *J. Biol. Chem.* **282**, 18980–18990
55. Alonso, G., Koegl, M., Mazurenko, N., and Courtneidge, S.A. (1995) Sequence requirements for binding of Src family tyrosine kinases to activated growth factor receptors. *J. Biol. Chem.* **270**, 9840–9848
56. Bourette, R.P., Arnaud, S., Myles, G.M., Blanchet, J.P., Rohrschneider, L.R., and Mouchiroud, G. (1998) Mona, a novel hematopoietic-specific adaptor interacting with the macrophage colony-stimulating factor receptor, is implicated in monocyte/macrophage development. *EMBO J.* **17**, 7273–7281
57. Roussel, M.F., Shurtleff, S.A., Downing, J.R., and Sherr, C.J. (1990) A point mutation at tyrosine-809 in the human colony-stimulating factor 1 receptor impairs mitogenesis without abrogating tyrosine kinase activity, association with phosphatidylinositol 3-kinase, or induction of c-fos and junB genes. *Proc. Natl. Acad. Sci. USA* **87**, 6738–6742
58. Mendel, D.B., Laird, A.D., Xin, X., Louie, S.G., Christensen, J.G., Li, G., Schreck, R.E., Abrams, T.J., Ngai, T.J., Lee, L.B., Murray, L.J., Carver, J., Chan, E., Moss, K.G., Haznedar, J.O., Sukbunthorn, J., Blake, R.A., Sun, L., Tang, C., Miller, T., Shirazian, S., McMahon, G., and Cherrington, J.M. (2003) In vivo antitumor activity of SU11248, a novel tyrosine kinase inhibitor targeting vascular endothelial growth factor and platelet-derived growth factor receptors: determination of a pharmacokinetic/pharmacodynamic relationship. *Clin. Cancer Res.* **9**, 327–337
59. Wodicka, L.M., Ciceri, P., Davis, M.I., Hunt, J.P., Floyd, M., Salerno, S., Hua, X.H., Ford, J.M., Armstrong, R.C., Zarrinkar, P.P., and Treiber, D.K. (2010) Activation state-dependent binding of small molecule kinase inhibitors: structural insights from biochemistry. *Chem. Biol.* **17**, 1241–1249
60. Gajiwala, K.S., Wu, J.C., Christensen, J., Deshmukh, G.D., Diehl, W., DiNitto, J.P., English, J.M., Greig, M.J., He, Y.A., Jacques, S.L., Lunney, E.A., McTigue, M., Molina, D., Quenzer, T., Wells, P.A., Yu, X., Zhang, Y., Zou, A., Emmett, M.R., Marshall, A.G., Zhang, H.M., and Demetri, G.D. (2009) KIT kinase mutants show unique mechanisms of drug resistance to imatinib and sunitinib in gastrointestinal stromal tumor patients. *Proc. Natl. Acad. Sci. USA* **106**, 1542–1547
61. Mashkani, B., Griffith, R., and Ashman, L. K. (2010) Colony stimulating factor-1 receptor as a target for small molecule inhibitors. *Bioorg. Med. Chem.* **18**, 1789–1797